Revista Mexicana de Física
ISSN: 0035-001X
rmf@ciencias.unam.mx
Sociedad Mexicana de Física A.C.
México

Landa, E.; Fossion, R.; Morales, I.; Hernández, C.; Velázquez, V.; López Vieyra, J.C.; Frank, A.
Fractal scale invariance in chaotic time series: classical and quantum examples
Revista Mexicana de Física, vol. 55, núm. 2, 2009, pp. 50-59
Sociedad Mexicana de Física A.C.
Distrito Federal, México

Fractal scale invariance in chaotic time series: classical and quantum examples

E. Landa[a], R. Fossion[a], I. Morales[a], C. Hernández[a], V. Velázquez[b], J.C. López Vieyra[a], and A. Frank[a]
[a]*Instituto de Ciencias Nucleares, Universidad Nacional Autónoma de México.*
[b]*Facultad de Ciencias, Universidad Nacional Autónoma de México,*
México, D.F., 04510, México.

Recibido el 14 de junio de 2009; aceptado el 16 de junio de 2009

Important aspects of chaotic behaviour appear in systems of low dimension, as illustrated by the Logistic Map. It is indeed a remarkable fact that all systems that make a transition from order to disorder by the period-doubling route, display common properties, irrespective of their exact functional form. We discuss preliminary evidence for $1/f$ power spectra in the chaotic time series associated with the Logistic Map, as a mathematical model for the dripping faucet that can be seen as a paradigm for classical chaos. In the same context, we also consider a new experiment with photons that constitutes what we call a "dripping laser". We discuss the possible consequences of these preliminary analyses.

Keywords: Time-Series Analysis; fluctuatio phenomena; random processes and Brownian motion; noise; nonlinear dynamics and chaos; photon statistics and coherence theory; dynamics of nonlinear optical systems; optical chaos and complexity; optical spatio-temporal dynamics; Fourier analysis.

Aspectos importantes del comportamiento caótico aparecen en sistemas de dimensión baja, según lo ilustrado por el mapeo logístico. Es un hecho notable de que todos los sistemas que hagan una transición de orden al desorden por la ruta de duplicación de período, muestran propiedades comunes, independientemente de su forma funcional exacta. Discutimos evidencia preliminar para espectros de potencias $1/f$ en las series de tiempo caóticas asociadas al mapeo logístico, como modelo matemática para el grifo goteante que se puede ver como paradigma para el caos clásico. En el mismo contexto, consideramos un nuevo experimento con fotones que constituye lo que llamamos un "laser goteante". Discutimos las posibles consecuencias de estos análisis preliminares.

Descriptores: Análsis de series de tiempo; fenómenos de fluctuaciones procesos aleatorios y movimiento Browniano; ruido; dinámica no-lineal y caos; estadística de fotones y teoría de coherencia; dinámica de sistemas ópticos no-lineales; caos óptico y complejidad; dinámica óptica espacial-temporal; análisis de Fourier.

PACS: 05.45.Tp; 05.40.-a; 02.50.-r; 05.40.Ca; 05.45.-a; 42.50.Ar; 42.50.Md; 42.65.Sf; 02.30.Nw

1. Introduction

Classical chaos, is understood as a non-linear phenomenon, which gives rise to an *unpredictable* time-evolution of the corresponding dynamical systems. In particular, it is characterized by an intrinsic instability in the orbits due to a high sensitivity to initial conditions. This is not to say that the physics describing the system is wrong, in fact, the physics predicts this chaotic motion, it is just extremely sensitive to the initial state of the system. In general, the dynamical instability of the orbits in a chaotic system is accompanied by the occurrence of strange attractors with a fractal structure in phase space.

The concept of *quantum chaos* [1] has no unique or precise definitio as yet. Quantum chaos is often understood as the study of quantum manifestations of classical chaos. One of the characteristics of classical chaos is the sensitivity to the initial conditions, something which is not observed in quantum mechanics because it is a linear theory. However, both in classical and in quantum chaos "patterns of order in disorder" can be found: in classical chaos in terms of (strange) attractors in the dynamics, in quantum chaos universal laws have been proposed for the behaviour of fluctua tions in excitation spectra [2]. More in particular, it has been established that there is a relationship between energy-level fluctuation-propertie of a quantum system and the dynamics of its classical analog [2]. Quantum systems that have a classical analog that is chaotic, have spectral fluctuation that show a strong repulsion between energy levels and follow the predictions of Random-Matrix Theory (RMT) [3] (there are some counterexamples, such as arithmetic billiards [4]). On the other hand, quantum systems that have a classical counterpart that is integrable, give rise to an energy spectrum, in which the fluctuation are uncorrelated, and that have a nearest-neighbour spacing distribution that is well described by Poisson statistics [5].

The notion of *scale invariance* appears in many different phenomena. For example, in second-order phase-transitions, it appears near the so-called *critical points* where some physical quantities obey a power-law behaviour. In paricular, the correlation lenght^i ξ behaves like $\xi \sim |T - T_{crit}|^{-\nu}$, with ν being the corresponding *critical exponent*. At the critical temperature, the correlation lenght ξ diverges and the system has no characteristic scale, *i.e.* the system becomes scale invariant. In particular, the correlation function behaves as $\Gamma(r) \sim r^{-p}$. The analog for T_{crit} in the case of a quadratic map is the control parameter $k \rightarrow k_\infty$, where k_∞ is the period-doubling critical point and where all cycles of period 2^n with $n = 0, 1, 2, \ldots$, are unstable. The instability of cycles of arbitrarily long period is superficiall analogous to the role played by divergent fluctuation in critical phenomena.

Power-law behaviour has been observed in the study of many different chaotic time series, for example in the problem of a dripping faucet [7], in heartbeat dynamics [8] and in a large variety of other phenomena.

Recently, it was found that the power spectrum of the fluctuation of the eigenvalues of RMT ensembles and nuclear shell-model Two-Body Random Ensemble (TBRE) calculations exhibit a power-law behaviour $\sim 1/f$ (with f being the frequency) [9], whereas, for the case of integrable systems the corresponding power spectrum behaves as $\sim 1/f^2$ [9]. This also implies a power-law behaviour of the auto-correlation function (Wienner-Khinchin theorem).

In this contribution, we present preliminary results that aim at a deeper understanding of the physical meaning of the exponent β in power spectra that behave like the power law $1/f^{\beta}$. To do so, in this contribution, we study the power spectra of the fluctuation of time series of two systems in transition between an uncorrelated and a correlated regime,

(i) the classical system of the Logistic Map, and

(ii) the quantum system of the "dripping laser", where a ground glass disc rotating in a laser beam permits us to realice a phase transition between the regime of uncorrelated laser light, and the regime of pseudothermal light where photons travel in drops or bunches.

This paper is organized as follows. In Sec. 2, we discuss the fractal and scale-invariance consequences of $1/f$-type power spectra. In Sec. 3, we study the classical example of the Logistic Map. In Sec. 4, we study the quantum example of the "dripping laser". In Sec. 5, we present our preliminary conclusions.

2. Fractality and scale invariance

The concept of a fractal is associated with geometrical objects satisfying two criteria: self similarity and fractional dimensionality. Self similarity means that an object is composed of units, sub-units and sub-sub-units on multiple levels that (statistically) resemble the structure of the whole object. A related property is scale invariance which can be thought of as self-similarity on all scales [10]. Thus, a fractal structure lacks any characteristic length scale. This fractal structure is seen, *e.g.*, in the bifurcation diagram of the logistic map, see Fig. 1. In particular, the auto-correlation function of a $1/f$ signal is scale independent, *i.e.* the auto-correlation function is fractal. A demonstration in the continuum case is the following: suppose that the power spectrum[ii] of a given time series has a $1/f$ behaviour, *i.e.*

$$\mathcal{S}(f) = 1/f. \tag{1}$$

Since the Fourier Transform of the power spectrum is identical to the autocorrelation function $\mathcal{C}(\tau)$ (Wiener-Khinchin Theorem) we have:

$$\mathcal{C}(\tau) = \mathcal{F}^{-1}(\mathcal{S}(f)) = \mathcal{F}^{-1}(1/f). \tag{2}$$

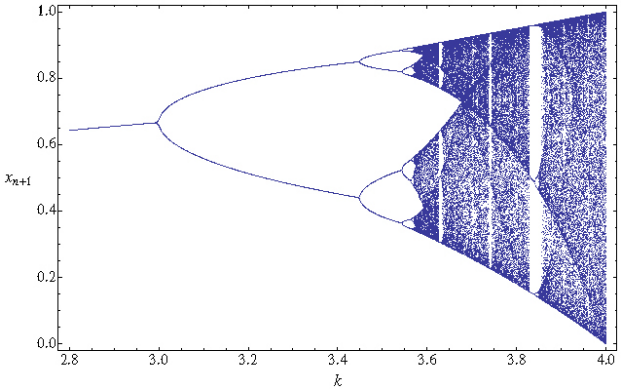

FIGURE 1. Bifurcation Diagram of the Logistic Map with control parameter $2.8 \leq k \leq 4.0$ [see Eq. (5)].

Now, if we make a scale transformation in the time domain we have

$$\mathcal{C}(a\tau) = \mathcal{F}^{-1}\left(\frac{1}{a}\left(\mathcal{S}(f/a)\right)\right) = \mathcal{F}^{-1}\left(\frac{1}{a} \times \frac{a}{f}\right). \tag{3}$$

Thus

$$\mathcal{C}(a\tau) = \mathcal{C}(\tau). \tag{4}$$

We have used the scaling property of Fourier Transforms, which is strictly valid only in the continuum case. For discrete time series, there are other tools for studying the scale invariant properties, including the Detrended Fluctuation Analysis (DFA) method [11]. The main result is then that a $1/f$ behaviour suggests scale invariance. In fact, $1/f$ behaviour (referred to as flic er or $1/f$ noise) occurs in many physical, biological and economic systems, meteorological data series, the electromagnetic radiation output of some astronomical bodies, and in almost all electronic devices. In biological systems, it is present in heart-beat rhythms and the statistics of DNA sequences. In financia systems, it is often referred to as a long-memory effect. In quantum systems, $1/f$ behaviour is found in quantum fluctuation of the spectra of random hamiltonians and of atomic nuclei [9, 12, 13]. There are even claims that almost all musical melodies, when each successive note is plotted on a scale of pitches, will tend towards a $1/f$ noise spectrum.

3. Logistic map

Our study of the logistic map was motivated by the study of a system that shows complex dynamical behaviour, namely the *dripping faucet*. The dripping faucet exhibits chaotic behaviour as the fl w rate is varied, firs conjectured by Rössler [14], and experimentally confirme afterwards by Shaw [15]. $1/f$ behaviour has also been suggested in the dripping faucet [7]. We have focused on the logistic map because it shows similar properties to the dripping faucet, such as period doubling, multiperiodicity, Hopf bifurcation, multiple stability, strange attractors and so forth. The Logistic Map is a one-dimensional map where the value x_{n+1} at step

$n+1$ depends explicitely only on the value x_n of the previous step n, with a relationship given by the equation,

$$x_{n+1} = kx_n(1 - x_n). \tag{5}$$

We will use the range $x \in [0, 1]$ and $0 < k \leq 4$, where k is called the control parameter, which plays a critical role to determine the dynamical behaviour of x_n vs. the discrete time steps n. In many applications, the map is a model for the dynamics of a population, where x_n is the size of the population of the *n*th generation. Robert May and others have shown that this map exhibits an astonishing range of behaviours, as the growth rate k is varied [16]. The logisitic map was studied by the mathematical physicist M. Feigenbaum in the 1970's. His discoveries include scaling laws for subsequent bifurcations: the ratio $(k_\ell - k_{\ell-1})/(k_{\ell+1} - k_\ell)$ approaches a constant δ for $\ell \to \infty$ (here k_ℓ is a value between $[0, 4]$ corresponding to the value of k where the ℓ-th bifurcation occurs), this constant is analogous to a critical exponent in the theory of phase transitions [17].

We study the dynamical behaviour of the Logistic Map analyzing a global representation on the various regimes that are encountered as the control parameter k is varied. This can be done with the help of bifurcation diagrams and also with Lyapunov exponents, which are tools commonly used in nonlinear dynamics. Bifurcation diagrams display some characteristic properties of the asymptotic solution of a dynamical system as a function of a control parameter, allowing one to see at a glance where qualitative changes in the asymptotic solution occur. Such changes are termed bifurcations. In our case we have a single dynamical variable, the bifurcation diagram is readily obtained by plotting a sample set of values of the sequence x_n as a function of the parameter k, as shown in Fig. 1.

If $0<k<3$, then the dynamics of x_n has a stable fi ed-point attractor, while for intermediate values, $3 < k < 3.569$ the dynamics of the x_n is periodic. Going on, for $3.569 < k < 4$, the dynamics of x_n is mostly chaotic, and it is in this range that we are mostly interested for our analysis. There are however, values of the control parameter in this range that lead to periodic behaviour of x_n. To exclude these periodic series $x_n(k)$, we calculate for each value of k the value of the Lyapunov exponent λ_k,

$$\lambda_k = \lim_{m \gg} \frac{1}{m} \sum_{n=0}^{m-1} \log \left| x'_{n+1} \right|, \tag{6}$$

where $x'_{n+1} = k(1-2x_n)$ is the derivative of x_{n+1} of Eq. (5) with respect to the previous value x_n. Periodic series give rise to a negative Lyapunov exponent, whereas chaotic series have a positive exponent. In what follows, we will thus concentrate only on series $x_{n+1}(k)$ with $\lambda_k > 0$. A similar approach has been followed in Ref. 18. The variety of behaviour displayed by the Logistic Map is easily explored, as illustrated in Fig. 2. One find quickly that two main types of dynamical behaviour can be observed: (i) stationary or periodic regimes on the one hand that we will exclude from our study (see upper panels), and (ii) chaotic regimes on the other hand (see lower panels). In the latter case, the state of the system never repeats itself exactly and seemingly evolves in a disordered way. We are interested in a study on how chaos evolves over the Logistic Map as a function of k, in particular, we want to investigate whether we can fin a specifi behaviour of the exponent β of the power spectrum of the time series associated to the Logistic Map.

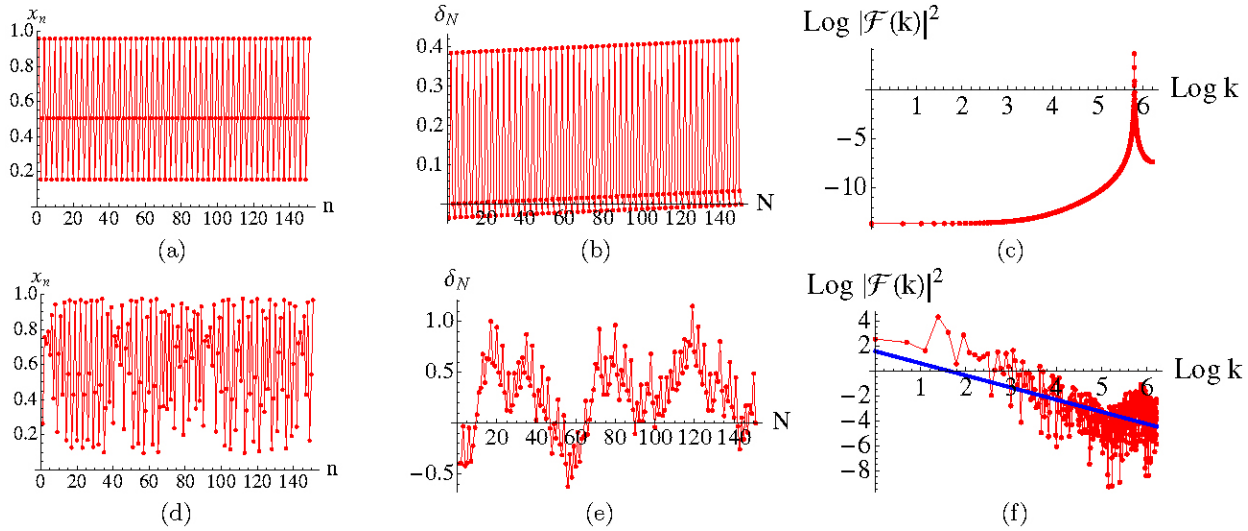

FIGURE 2. (Upper row) Dynamical regular behaviour in the Logistic Map with period 3 for $k = 3.83$ for (a) firs 150 values of the series of Eq. (5), (b) the fluctuation δ_N, and (c) the power spectrum in log-log scale with a linear fi that gives the exponent β as its slope. (Lower row) Dynamical chaotic behaviour for $k = 3.9$ for (d) firs 150 values of the series of Eq. (5), (e) the fluctuation δ_N, and (f) the power spectrum in log-log scale with a linear fi that gives the exponent β as its slope.

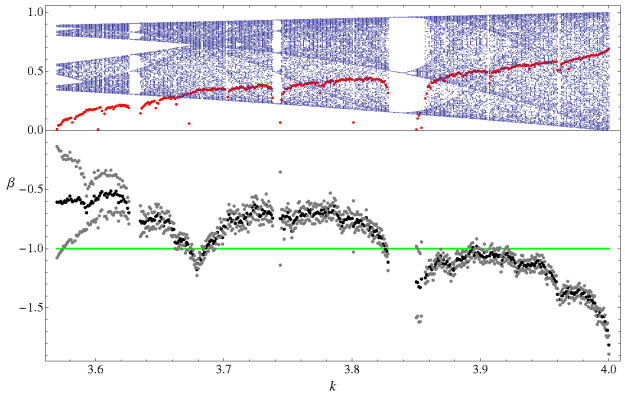

FIGURE 3. (Upper panel) Enlarged view of the chaotic zone of the bifurcation diagram of Fig. 2 with $3.5 \leq k \leq 4.0$ (small dots). Also shown are the Lyapunov exponents (large dots) for the series $x_n(k)$ for each k. (Lower panel) Slope β of a linear fi to the power spectrum of the statistical measure δ_N of the series $x_n(k)$ that have a positive (chaotic) Lyapunov exponent in the range $3.5 \leq k \leq 4.0$ (black dots). Also shown is the standard deviation for β for each k (grey dots).

3.1. Fluctuations in the Logistic-map time-series

In Ref. 18, a statistical study of the Logistic Map has been carried out, applying the Detrended Fluctuation Analysis (DFA) [11] technique on the *series of values* $x_n(k)$ [see Eq. (5)]. The conclusion of this study was that *series obtained from stochastic (noise-driven) and deterministic systems might be indistinguishable using the DFA method*. In literature, when *time series* are studied both in the classical (*e.g.* heart beats [8] or the dripping faucet [7]) as in the quantum world (*e.g.* the nuclear excitation spectrum [9]), what appears to be important are the *fluctuations* in the series and not the series itself. In these studies, there are indications that a system carrying out a phase transition between an ordered and a disordered regime, the power spectrum of the fluctua tions in the corresponding time series behaves like $1/f$ near the critical point where chaos is setting in. In the following, we want to test this idea on the Logistic Map, using k as a control parameter. To do so, the series of values x_n of the Logistic Map must be "translated" into a time series, of which the fluctuation can then be studied statistically. In our calculations; we used series of values x_{n+1} of dimension 1000 ($1 \leqq n \leqq 1000$) [see Fig. 2, panel (d)]. We defin a new series,

$$T_i = \sum_{n=1}^{i} x_n, \tag{7}$$

interpreting the value x_n as the analogue of the time interval between the nth and the $(n+1)$th drop of the dripping faucet. In the following analysis, we will treat T_i as a generalized discrete time. To obtain the fluctuation of this time series, we need to subtract the smooth global behaviour, a process coined *unfolding*. In this case, the smooth behaviour is a straight line, $\overline{T}_i$. The fluctuation of the time series of the Logistic Map can thus be define as,

$$\delta_N = \sum_{i=1}^{N} [T_i - \overline{T}_i]. \tag{8}$$

The discrete function δ_N measures the fluctuation in the time series of the Logistic Map with respect to the corresponding uniform (equally spaced) time series $\overline{T}_i$ [see Fig. 2, panel (e)]. The statistical measure δ_N was firs proposed by Relaño and collaborators [9], and has been applied by some of us [12], to translate the series of energies in a nuclear excitation spectrum into a time series and to obtain its fluctuation with respect to a uniform (equally spaced) spectrum.

3.2. Conclusions

In our calculations, we used series of values $x_n(k)$ of dimension 1000, for which we calculated the power spectrum for the fluctuation in the associated time series $\delta_N(k)$ [see Fig. 2, panel (f)]. We found that the exponent $\beta(k)$ of the power spectrum does not change much with the dimension of the original series of values. Also, the dispersion in the power spectrum of a time series can be diminished calculating a mean power spectrum averaging over many power spectra of parts of the original time series, but the value of the exponent β does not change significantl . In Fig. 3, we show the evolution of the exponent $\beta(k)$ (lower panel) for values of the control parameter k where the Lyapunov exponent is positive (upper panel), see Eq. (6). It can be seen that the requirement $\lambda_k > 0$ indeed removed the periodic windows from the bifurcation diagram. The value of the exponent β can be seen as a measure of the correlations that are present in the dynamical system. The limiting values of the exponent are $\beta = 0$ when no correlations are present in the system (white noise), and $\beta = -2$ when the correlations are maximum (brown noise). In between these limiting values, $\beta = -1$ or $1/f$ noise, has been proposed as a particularly behaving system showing a fractal scale-invariant autocorrelation function (see Sec. 2). In Fig. 3, $\beta(k)$ would seem to have a particular behaviour with control parameter k, oscilating around the value -1. There must be a connection between the behaviour of $\beta(k)$ and the strange attractors of the Logistic Map, that we can recognize in the bifurcation diagram of Fig. 3 (upper panel) as "boundaries" or high-density lines [20, 21]. For the particular value of the control parameter $k = 4.0$, as stated in Ref. 21, *there are no remaining boundaries to confine the dynamics of the map, so the attractor becomes infinite, and is destroyed*. This results in a random series of values x_{n+1}. The cumulative statistics δ_N (see Eq. 8) translates a random series in a highly-correlated series. Thus in the case for $k \to 4.0$ we can understand that $\beta(k) \to -2$. The behaviour of $\beta(k)$ with k clearly deserves a more thorough study, see Ref. 19. A problem in this study is that the power spectra do not always behave perfectly like a $1/f^{\beta}$ power-law [see Fig. 3 (f)], so that it is not always possible to defin the power spectrum by one single value, *i.e.* the value of its exponent β. In a future study [19], we want to

check our results for the Logistic Map with the more correct but more tedious formulation for the Lyapunov exponent,

$$\lambda_k = \lim_{\epsilon\to 0, n\gg} \frac{\Delta x_n}{\Delta x_0} = \lim_{\epsilon\to 0, n\gg} \frac{x_n^k(x_0+\epsilon) - x_n^k(x_0)}{\epsilon}. \quad (9)$$

In particular, we want to understand the relation between $\lambda(k)$ and $\beta(k)$, that is not clear yet.

4. Phase transition in light

4.1. Different types of light

Light from different sources can have different properties. Lasers emit *coherent* light, in which the time intervals between the successive photons are uncorrelated and fluctuatin around a mean time interval, but in which all photons travel in phase. Also the number of photons n that is detected per fi ed time interval T will fluctuat around a mean number $\overline{n}$, resulting in a histogram that obeys the Poisson distribution [22],

$$P_P(\overline{n}, n) = \frac{\overline{n}^n e^{-\overline{n}}}{n!}. \quad (10)$$

Light from thermal sources is called *thermal* light, and has the property that photons are grouped or *bunched* in packages with very small time intervals between the constituent photons, separated from the other packages or bunches by much larger time intervals. Because of the bunching effect, a time series of time intervals between photons of bunched light will show correlations. A histogram of the photon count n per fi ed time interval T will now obey the Bose-Einstein distribution [22],

$$P_{BE}(\overline{n}, n) = \frac{\overline{n}^n}{(\overline{n}+1)^{n+1}}. \quad (11)$$

When photons are produced individually in nonlinear crystals by descending or ascending parametric conversion [23, 24], the resulting light is called *quantum light*, and shows *antibunching*, which means that photons will avoid to form groups.

Thermal light has the property that its *coherence time* (the duration in time of a package or bunch of photons) is very small, shorter than 10ns, and thus the properties of thermal light are very hard to study experimentally. It is possible to simulate thermal light, called *pseudothermal* light, with a ground glass disc that is rotating with an adjustable speed in the light beam of a laser [22, 25]. The dispersion of the laser light from the irregularities of the ground glass disc will create packages or bunches of photons with larger coherence times, up to the microsecond or millisecond regime, depending on the velocity of the glass disc, making pseudothermal light available for experimental study. The irregularities should be uniformly distributed over the surface of the disc, to avoid spurious effects that the rotation of non-uniform regions of the disc could introduce in the light passing through it. The light produced by this experimental setup is called pseudothermal because it has photons of only one wavelenght (the wavelength at which the laser emits), whereas a thermal source emits black-body radiation with a continuous distribution of wavelenghts.

4.2. Phase transition in light

In literature, one distinguished usually between coherent and (pseudo)thermal light calculating photon-count histograms that behave like the Poisson or the Bose-Einstein distribution, respectively. When the ground glass disc is standing still, the laser light passing through it will still be coherent. The statistics will not change, and only the intensity of the beam will be attenuated. We checked the photon counting statistics for several fi ed time intervals T, and the histogram obeys the Poisson statistics typical for coherent light. Experimentally, we calculated the mean photon count $\overline{n}$ per counting interval T, and used this number to calculate the Poisson and Bose-Einstein distributions of Eq. (10) and Eq. (11). In Fig. 4 (upper panel) we show the results for a fi ed counting

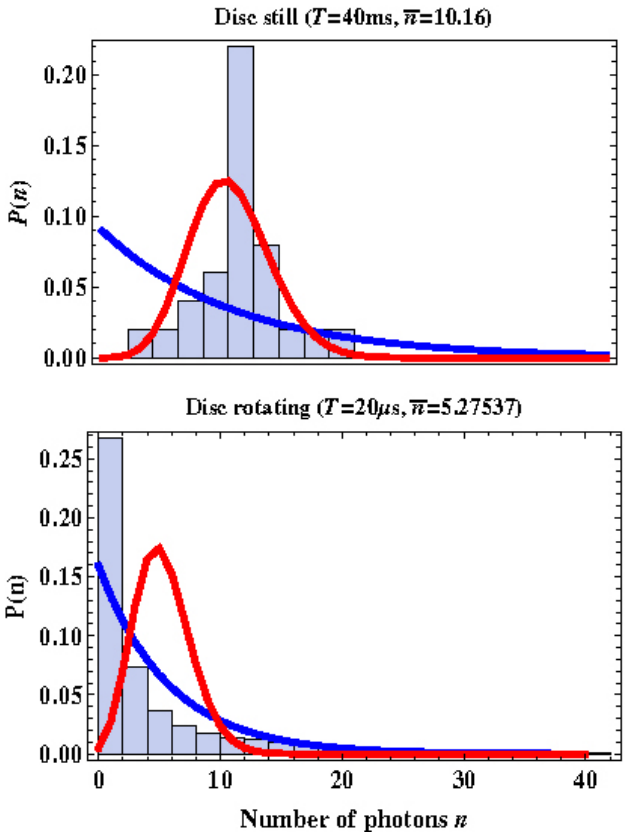

FIGURE 4. Histogram of the number of photons n detected per fi ed counting interval T, compared with the Poisson (continuous line) and the Bose-Einstein (dashed line) distributions. (Upper panel) The case of the glass disc standing still and for a fi ed counting interval $T = 40$ms, the mean number of photons arriving per interval T is $\overline{n} = 10.16$. (Bottom panel) The case of the glass disc rotating with a frequency of $\nu = 38.46$Hz, and for a fi ed counting interval of $T = 20\mu$s, the mean number of photons arriving per interval $\overline{n} = 5.28$.

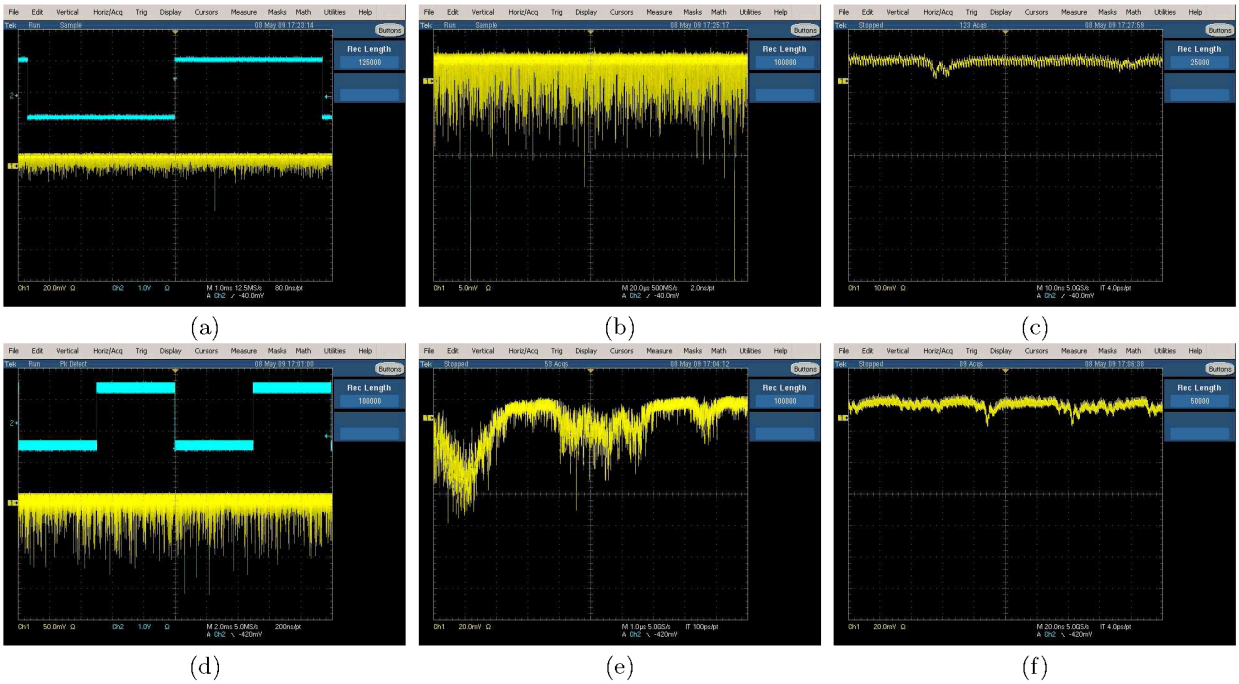

FIGURE 5. A fotomultiplier tube produces a voltage drop V_i when it detects a photon. This time signal (t_i, V_i) can be observed with an osciloscope. (Upper row) For coherent laser light, the time series is random at all resolutions. (a) Random time series for a screen width of 10ms, (b) random time seires for a screen width of 200μs, and (c) the typical signal for a single photon or simultaneous photons for a screen width of 100ns. (Lower row) Pseudothermal light at poor resolutions is observed as random coherent light. At appropriate resolutions, photon bunches can be observed. (d) Random time series for a screen width of 20ms, (e) photon bunch with a width of a few μs observed for a screen width of 10μs, and (f) the typical signal for a single photon or simultaneous photons for a screen width of 200ns. An external quadratic function [see panels (a) and (d)] was used to help the osciloscope to write the data (V_i, t_i) to fil after equal time intervals.

interval of $T = 40$ms. When the disc is rotating, bunches will be formed, and the counting statistics will obey the Bose-Einstein statistics. In fig 4 (bottom panel), we show the results for a rotating speed of our disc of $\nu = 38.5$Hz and for a counting interval of $T = 20\mu$s. The agreement between the experimental histograms and the theoretical distributions could be improved using longer experimental time series. It must be possible to realise a phase transition in light, from the coherent regime to the pseudothermal regime, using the rotation speed of the disc as an (external) control parameter. The study of this phase transition will be the subject of a forthcoming publication [26]. In the present study we will use a single specifi and constant speed for our disc (in this case $\nu = 38.5$Hz). We want to understand better the statistics of the series of photons counts, now interpreted as a *time series*, using a power-spectrum analysis.

4.3. Series of photon counts per time interval T as a time series

In our experiment, we use a photomultiplier tube to detect the photons of the coherent or pseudothermal light beams. When the photomultiplier detects a photon, it produces a voltage drop. This time signal can be observed with an osciloscope. The osciloscope shows a new data point, voltage vs. time (V_i, t_i), every 80ns. Coherent light observed with the osciloscope is random at all time scales, see Fig. 5 (upper panels). Pseudothermal light, on the other hand, at poor resolutions looks like random coherent light, but shows bunches of photons at the correct resolutions (see bottom panels). The width of a photon bunch gives an empirical measure for the coherence time τ_{coh} of the observed pseudothermal light. In this experiment, we found that the bunches had a typical width of a few microseconds. By constructing histograms of photon counts, as one does traditionally in literature to distinguish between coherent and pseudothermal light (see Fig. 4), one loses information on how the system behaves in time (see Fig. 5). In the following, we will consider the series of photon counts n per fi ed counting interval T as a time series. How the series of photon counts per time interval T looks, also strongly depends on the resolution (the size of the counting interval T relative to the mean time interval $\overline{\Delta t}$ between the successive photons). In this experiment, we found $\overline{\Delta t} = 3.79\mu$s. This corresponds to the coherence time τ_{coh} we observed emperically with the osciloscope. For a large counting interval, *e.g.* $T = 10$ms, no bunches will be observed, and the photon count number n will be found fluc tuating around a certain mean $\overline{n}$, see Fig. 6 (upper panel). Using smaller time intervals, but still orders of magnitude larger than $\overline{\Delta t}$, *e.g.* $T = 1$ms (middle panel), we observed peaks in the counting time series, but they were most probably produced artificiall by the rotation of the disc $\nu = 38.46$Hz and the periodic motion of a small number N of regions of

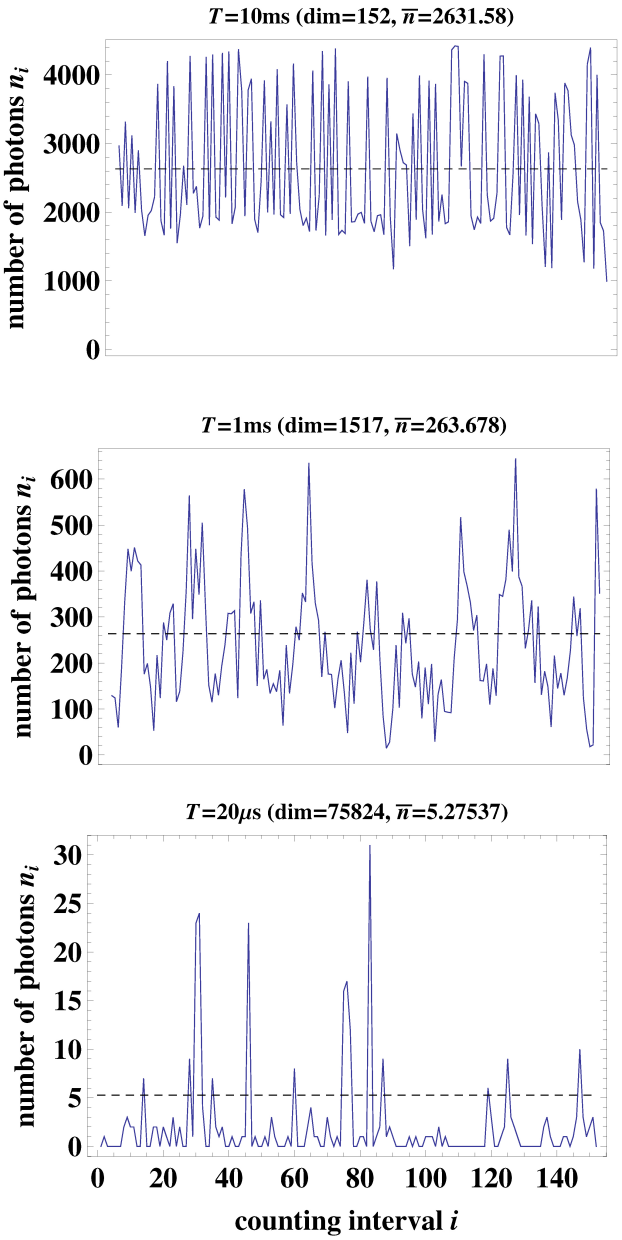

FIGURE 6. Listplots of the time series of photon counts n_i per successive equal time intervals of $T = 10$ms (upper panel), $T = 1$ms (middle panel) and $T = 20\mu$s (lower panel). It can be appreciated that series of photon counts evolves from fluctuation around the mean count (left panel) to a peaked behaviour (middle and right panel). In this experiment, the mean time interval between successive photons was 3.79μs.

non-uniformities, that will pass every time interval t=1/N $\times$ 1/38.46Hz=26/Nms in front of the pinhole of the photomultiplier. When plotting the data points (t_i, V_i) of a number of file saved by the osciloscope, see Fig. 7, we fin structures with a width of about 10ms for pseudothermal light (bottom panel), whereas a similar plot for coherent light looks completely random (upper panel). When the counting interval T becomes of the order of the mean photon time-interval $\overline{\Delta t}$ or the coherence time of the bunch τ_{coh}, the bunches of the pseudothermal light pop up in the series of photon counts as large peaks in between much smaller photons counts (see Fig. 6, lower panel). The resolution, or the relative size of the counting time interval T can be seen as some sort of internal control parameter that lets us see a phase transition within the same time series, in between coherent light (with a photon count fluctuatin around the mean count) and pseudothermal light (with bunches of high counts in between much smaller counts).

4.4. Power spectrum

We can use the discrete Fourier Transform to study the behaviour of the power spectrum of the series of photon counts interpreted as a time series, using the resolution power of the count time-interval T to see how the power spectrum will

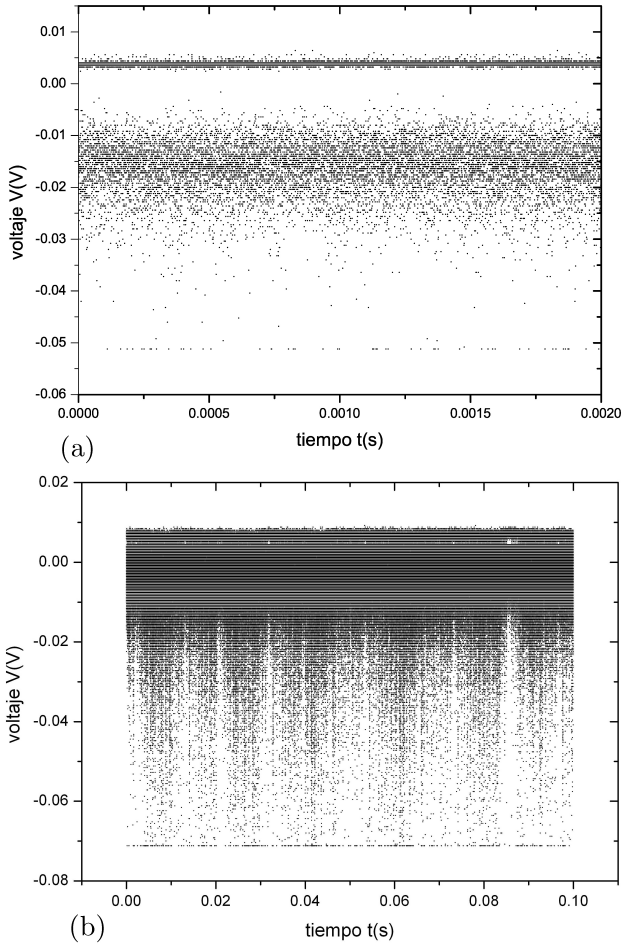

FIGURE 7. The osciloscope writes a data point (t_i, V_i) every 80ns, *i.e.* the voltage observed in the fotomultiplier tube vs. time. In total, we recorded 340 data file for coherent light and 500 data file for pseudothermal light. Each data fil contains 125000 data points. A representation of this time series shows that (a) for laser light it is random, and that (b) for pseudothermal light coming from the rotating disc it is organised in structures of some 10ms in width. Only a part of the data is represented (1% in the case of the coherent light and 2% in the case of pseudothermal light), we made sure that the figure are representative for the totality of the data.

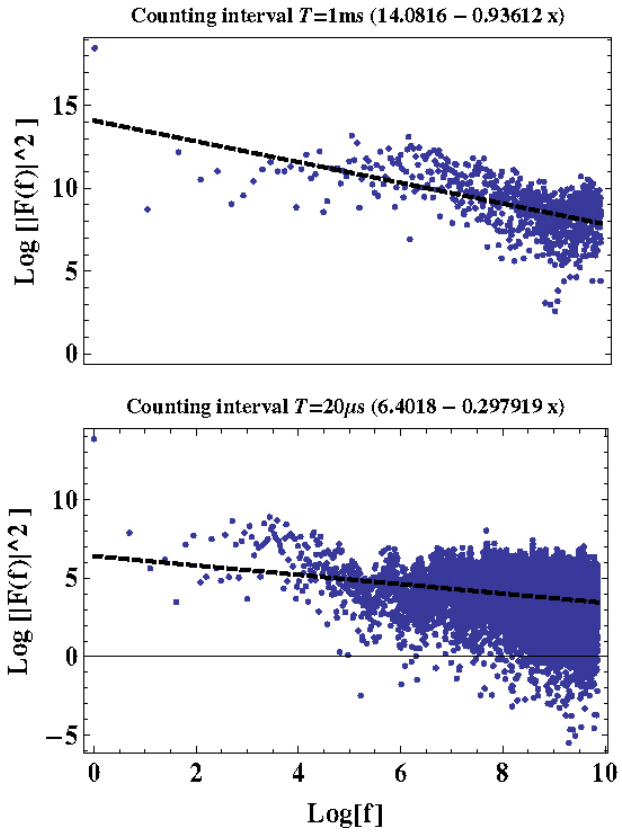

FIGURE 8. Power spectrum $|F(f)|^2$ vs. frequency f in a log-log representation for the series of photon counts per fi ed counting interval T. (Upper panel) For counting interval $T = 1$ms, giving a linear fi with slope $\beta = -0.936$. (Bottom panel) For counting interval $T = 20\mu$s, giving a linear fi with slope $\beta = -0.298$.

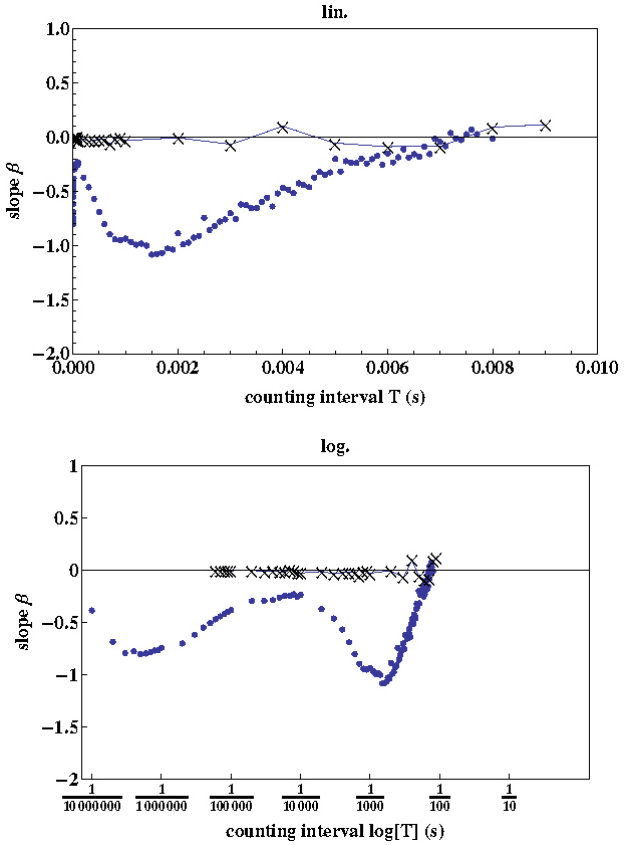

FIGURE 9. Dependence of the slope β of a linear fi to the power spectrum of series of photons counts per fi ed counting interval T, as a function of this counting interval, in the case of the glass disc standing still (connected crosses) and the disc rotating with a frequency $\nu = 38.46$Hz (connected). The counting interval T is represented in linear scale (upper panel) and in logarithmic scale (bottom panel). The function $\beta(T)$ for coherent light is not followed down to as small counting intervals T as for pseudothermal light because of the more tedious calculations. Coherent light is trivially scale invariant, $\beta(T) = 0$, whereas the pseudothermal light in this experiment shows specifi $1/f$ correlations in the time scale $T \sim$ ms, and close-to $\beta = -1$ correlations in the time scale $T \sim \mu$s.

change. The power spectra for two specifi cases are shown in Fig. 8, for $T = 1$ms (upper panel) and $T = 20\mu$s (bottom panel), together with a linear fi that gives us slopes $\beta = -0.936$ and $\beta = -0.298$, respectively. Similar to the analysis in Sec. 3B, the dispersion in the power spectra could be diminished calculating a mean power spectrum averaging over power spectra of smaller parts of the time series. We checked however that the value of β does not change significantly. It can be interesting to study the behaviour of the slope of the linear fi to the power spectrum of the series of photons counts per fi ed counting interval T as a function of this counting interval, in between the maximal values of the slope of $\beta = 0$ (no correlations or completely random behaviour), $\beta = -1$ (the conjectured fingerprin of classical and/or quantum chaos) and $\beta = -2$ (maximal correlation such as in the case of the brownian motion of the drunkard). This is shown in Fig. 9, in which we follow the behaviour of slope β with resolution T (the internal control parameter),

(i) for the disc standing still (connected crosses), and

(ii) the disc rotating with the constant speed $\nu = 38.46$Hz.

In this plot, the value of the exponent β will be constrained in between the limiting values $\beta = 0$ of a non-correlated time series, and $\beta = -2$ of a maximum-correlated time series. It is instructive to present both experimental cases of coherent light and pseudothermal light in the same figur because in this way the different nature of the two systems is put into evidence. The coherent light from he laser is uncorrelated, and gives $\beta = 0$ at all time scales T. Coherent light is thus trivially scale independent. For pseudothermal light, the case is different. For large counting intervals $T > 6$ms, we fin a slope $\beta = 0$, which means that at these poor resolutions T we observe the pseudothermal light as uncorrelated coherent light. When one counts per fi ed counting intervals T that are too large, the time series of photon counts will be very small and it makes no sense to calculate a power spectrum. Then, for $T < 6$ms, the slope β becomes more and more negative, obtaining the minimum value $\beta = -1$ in a broad plateau 0.8ms$< T <$2ms. This might be the effect of a small number

N of regions with non-uniformities in the disc that is rotating in the laser light at the specifi frequency of ν =38.46Hz. The regions with non-uniformities might create artificia patterns that have a period of $t = 1/N \times 1/38.46$Hz=$26/N$ ms, and probably correspond to the structures that we already saw in the case of pseudothermal light in Fig. 7 (bottom panel). These structures are of the scale of ms and thus of the same time scale as the $\beta = -1$ plateau in the $T \sim$ ms region. The disc has a constant rotation speed, but the number of photons that passes the disc per unit of time is random. If it is the interplay between the constant disc speed and the random number of photons that produces this plateau in the function $\beta(T)$, then it deserves more investigation why the power spectrum behaves like $1/f$ [26]. For counting intervals $T < 0.8$ms, the slope β become less negative (loss of correlation) up to $\beta = -0.3$: we are looking beyond the artificia correlations introduced by the rotating non-uniformities of the disc. The slope $\beta = -0.3$ persists down to $T = 100\mu$s, indicating minimal correlations. Then, when the counting interval becomes finall of the order of the coherence time of the photon bunches of the order of μs, the slope β becomes more negative again. The maximally negative value that we calculated in this region was $\beta = -0.8037$ for $T = 0.5\mu$s, very close to the $\beta = -1$ value of $1/f$ noise that gives rise to time series that have a fractal scale-invariant autocorrelation function. The time scale $T = 0.5\mu$s is indeed in correspondence with the coherence time we already found for the photon bunches, $\tau_{coh} \sim \mu$s [see Fig. 5, panel(e)]. For such small counting intervals T, the time series of photon counts becomes extremely large and, as a consequence, the calculation of the power spectrum becomes prohibitively tedious. The calculation of the value of β in the region of $T < 3\mu$s, was based on only a few percent of the available data. It is possible that the precise value of the β minimum in this region shifts somewhat if more data is included. Then, for even smaller counting intervals T, the slope β rises again and goes towards zero, indicating that the time scale goes beyond the correlation time inside a photon bunch.

4.5. Conclusions

We used a setup with a ground glass disc rotating in a beam of coherent laser light, with the goal to realise a phase transition in light between the coherent and the pseudothermal regime. When the disc stands still ($\nu = 0$Hz), coherent light is observed with photons that are not correlated in time between each other. When the disc is rotating ($\nu > 0$Hz), pseudothermal light is observed with photons that are grouped together or bunched. This experiment might be considered as a quantum equivalent for the dripping faucet, and thus we have it nicknamed as the *dripping laser*. The coherence time of the bunches is related to the rotation speed of the disc. In the phase transition between these two regimes of light, coherent and pseudothermal, the rotation speed of the disc can serve as an (external) control parameter. A thorough study of this phase transition as a function of the speed of the disc will be the subject of a future study [26]. In the second part of this contribution, we analyzed and compared the power spectra of the time series of photon counts per fi ed counting interval T, $(n_1, n_2, n_3, \ldots)$, for two cases:

(i) in the coherent regime with the disc standing still, and

(ii) in the pseudothermal regime with the disc rotating at the constant speed of $\nu = 38.46$Hz.

We found that the counting interval T could serve as an (internal) control parameter. In the case of pseudothermal light, the $1/f^{\beta}$ power-law behaviour of the power spectrum depends on the resolution of the counting interval T with the mean time-interval between the successive photons $\overline{\Delta t}$. More in particular, for low resolutions ($T \gg \overline{\Delta t}$), pseudothermal light is observed as coherent light without correlations ($\beta = 0$). Non-zero, negative values of β however, reveal at what time scales correlations between the photons show up. In particular, we found minima for β, close to $1/f$, both in the ms and in the μs time scale. We interpret the minimum for $T \sim \mu$s as *intrinsic*, that is to say, coming from the irregularities in the ground glass disc that disperse that light and that are responsible for the bunching effect. We interpret the minimum for $T \sim$ ms as *artificial*, meaning that it comes from the periodic motion of the disc. A future study [26], where we will study the angular velocity of the disc as an external control parameter, will make it probably possible to confir these interpretations. For coherent light, $\beta(T) = 0$ and its time series is uncorrelated at all time scales. We want to understand better the physical meaning of the parameter β, in between its limiting values $\beta = 0$ (uncorrelated time series) and $\beta = -2$ (maximally correlated time series), and whether the specifi value of $\beta = -1$ can be considered as the signature of a critical point at which chaos starts to set in. We expect that the study of a system in transition between a random and a correlated regime, such as the dripping laser, might offer us more insight.

5. Conclusions on fractal scale invariance in chaotic time series

It was shown that the fluctuation in the spectrum generated by the logisitc map exhibit non-trivial scale invariance (fractal or self similar). This scaling behaviour of the energy fluctuation has been observed in random shell model (TBRE) calculations as well as in shell model calculations with realistic interactions in the spectrum of ^{48}Ca, also in RMT [9, 12]. Since scale invariance is observed in several classical chaotic phenomena, as well as in phase transitional critical points (geometrical fractals, dripping faucet experiments, etc.), this result suggests a possible underlying connection between classical and quantum chaos. This is an open question which we shall continue to investigate.

We produced experimentally pseudothermal light using the setup with a rotating ground glass disc of Refs. 22 and 25, with a coherence time of some microseconds, to compare

its statistical properties with those of coherent laser light. Usually, histograms of the photon counts per fi ed counting time-interval are used to distinguish between both types of light: histograms of photon counts (pseudo)thermal light follow the Bose-Einstein distribution, whereas histograms of photon counts of coherent light follow the Poisson distribution. We interpret the series of photon counts per fi ed time interval T however as a time series, and use their power spectra as a statistical tool to analyse them. We use the counting time interval T as an internal control parameter (the resolution with which the time series is studied), and fin that the slope of a linear fi to the power spectra behaves very differently with T in the two cases. More in particular, $\beta(T) = 0$ independently of the time resolution T in the case of coherent laser light, indicating that it is uncorrelated at all time scales (trivially time-scale independent). For (pseudo)thermal light however, $\beta(T)$ starts at 0 for poor resolutions, but develops clear minima that indicate time scales with maximal correlation. A more thorough study is underway [26].

Acknowledgments

This work was supported in part by PAPIIT-UNAM and Conacyt-Mexico. We wish to thank M. Procopio, M. Grether, E. López-Moreno, E. Patiño, O. Rosas, and Alfred U'Ren for practical help and valuable discussions. We are also grateful to L. Benet for his most useful comments.

---

i The correlation lenght ξ is related to the behaviour of the correlation function $\Gamma(r)$. Near a critical point, the correlation function has the Ornstein-Zernike form $\Gamma(r) \sim r^{-p}e^{-r/\xi}$ when $T \to T_{crit}$ (see *e.g.* Ref. 6).

ii For a given time series δ_n, the power spectrum is define as $S(f) = |\mathcal{F}_f\{\delta\}|^2$, where $\mathcal{F}_f\{\delta\}$ denotes the component of the discrete Fourier transform of δ, having frequency f.

1. H.-J. Stoeckman, *Quantum Chaos*, 2nd ed. (Cambrige University Press, Cambrige, UK, 1999).
2. O. Bohigas, M.-J. Giannoni, and C. Schmit, *Phys. Rev. Lett.* **52** (1984) 1.
3. Mehta M.L., *Random Matrices*, 2nd ed. (Academic Press, New York London, 1991).
4. R. Aurich, M. Sieber, and F. Steiner, *Phys. Rev. Lett.* **61** (1988) 483; Bogomolny *et al.*, *Phys. Rev. Lett.* **69** (1992) 1477.
5. M.V. Berry and M. Tabor, *Proc. R. Soc. London A.* **356** (1977) 375.
6. K. Huang, *Statistical Mechanics*, Second Edition (John-Wiley and Sons 1987).
7. T.P.J. Penna, P.M.C. De Oliveira, J.C. Sartorelli, W.M. Goncalves, and R.D. Pinto, *Phys. Rev. E* **52** (1995) R2168.
8. A.L. Goldberger, D.R. Rigney, and BJ. West, *Chaos and fractals in human physiology. Sci. Am.* **262** (1990) 42.
9. A. Relaño, J.M.G. Gómez, R.A. Molina, J. Retamosa, and E. Faleiro, *Phys. Rev. Lett.* **89** (2002) 244102; *Phys. Rev. E* **66** (2002) 036209; E. Faleiro *et al.*, *Phys. Rev. Lett* **93** (2004) 244101.
10. R.J. Creswick, H.A. Farach, and C.P. Poole Jr. *Introduction to renormalization group methods in physics.*, First Edition (John-Wiley and Sons 1992).
11. C.-K. Peng *et al.*, *Phys. Rev. E* **49** (1994) 1685; C-K. Peng, S. Havlin, H.E. Stanley, and A.L. Goldberger, *Chaos* **5** (1995) 82.
12. E. Landa *et al.*, *Rev. Mex. Fís. S* **54** (2008) 48.
13. M.S. Santhanam, N.J. Bandyopadhyay, and D. Angom, *Phys. Rev. E* **73** (2006) 015201.
14. O.E. Rössler, *in Synergetics: A Workshop*, edited by H. Haken (Springer, Berlin, 1977), p. 174.
15. R.S. Shaw, *The Dripping Faucet as a Model Chaotic System* (Aerial, Santa Cruz, 1984).
16. R.M. May, *Nature* **261** (1976) 459.
17. J.L. McCauley, *Chaos, Dynamics and Fractals* (Cambrige University Press 1993).
18. M. Sozanski and J. Zebrowsky, *Acta Physica Polonica B* **36** (2005) 1803.
19. E. Landa *et al.*, in preparation.
20. Peitgen, Jörgens and Saupe, *Chaos and Fractals: New Frontiers of Science*, 2nd Edition (Springer, 2004); C. Grebogi, E. Ott, and J.A. Yorke, *Phys. Rev. Lett.* **48** (1982) 1507; J. Vandermeer and P. Yodzis, *Ecology* **80** (1999) 1817.
21. R.V. Jensen and C.R. Myers, *Phys. Rev. A* **32** (1985) 1222.
22. P. Koczyk, P. Wiewiór, and C. Radzewicz, *Am. J. Phys.* **64** (1996) 240.
23. A. Zavatta, S. Viciani, and M. Bellini, *Phys. Rev. A.* **70** (2004) 053821
24. A. Hayat, P. Ginzburg, and M. Orenstein, *Nature Photon.* **2** (2008) 238.
25. W. Martienssen and E. Spiller, *Am. J. Phys.* **32** (1964) 919.
26. R. Fossion *et al.*, to be published.